Endometrial stem cell-derived exosomes repair cisplatin-induced premature ovarian failure via Hippo/YAP pathway

Lijun Wang
the First Affiliated Hospital of Xi'an Jiaotong University
Lihui Wang
the First Affiliated Hospital of Xi'an Jiaotong University
Rongli Wang
the First Affiliated Hospital of Xi'an Jiaotong University
Ting Xu
the First Affiliated Hospital of Xi'an Jiaotong University
Jingyuan Wang
the First Affiliated Hospital of Xi'an Jiaotong University
Zhiwei Cui
the First Affiliated Hospital of Xi'an Jiaotong University
Feiyan Cheng
the First Affiliated Hospital of Xi'an Jiaotong University
Wei Wang
the First Affiliated Hospital of Xi'an Jiaotong University
Xinyuan Yang (1924484009@qq.com)
the First Affiliated Hospital of Xi'an Jiaotong University

Research Article

Keywords: chemotherapy, endometrial stem cells, exosomes, Hippo, YAP

Posted Date: July 11th, 2022

DOI: https://doi.org/10.21203/rs.3.rs-1656612/v2

Abstract

Background: Stem cells have been documented as a new therapeutic method for ovarian injuries such as premature ovarian failure (POF). However, effects of exosomes (Exos) derived from human endometrial stem cells (EnSCs) on diminished ovarian failure remain to be carefully elucidated. Our study aims to investigate the mechanisms of EnSC-Exos in the recovery of the cisplatin-induced granulosa cell injury model *in vitro* or POF mouses model *in vivo* and whether the Hippo signal pathway is involved in the regulation.

Methods: Exosomes derived from human EnSCs were isolated by ultracentrifugation and identified by electron microscopy and western blot (WB) analysis, stained by PKH26, respectively. The mechanism involving suppression of Hippo signaling pathway and activation of Yes-associated protein (YAP) was investigated for evaluating EnSC-Exos therapeutic effects in the cisplatin-induced granulosa cell injury model *in vitro* using flow cytometry, WB, qRT-PCR, immunofluorescence and EdU staining. Hematoxylin-eosin staining, ELISA and immunohistochemistry analysis were used for evaluating EnSC-Exos therapeutic effects in POF mouses model.

Results: In this study, we established successful construction of the cisplatin-induced granulosa cell injury model and evaluated Hippo signaling pathway activation in cisplatin-damaged granulosa cells (GCs). Furthermore, laser scanning confocal microscope and immunofluorescence demonstrated that EnSC-Exos can be transferred to cisplatin-damaged GCs to decrease apoptosis. In addition, the enhanced expression of YAP at the protein level as well as YAP/TEAD target genes, such as CTGF, ANKRD1 and the increase of YAP into the nucleus in immunofluorescence staining after the addition of EnSC-Exos to cisplatin-damaged GCs confirmed the suppression of Hippo signaling. While *in vivo*, EnSC-Exos successfully remedied POF in a mouse model.

Conclusions: Collectively, our findings suggest that human EnSC-Exos is effective in recovery of ovarian function by chemotherapy-induced POF via activating YAP and inhibiting the Hippo signaling pathway. These findings provide new insights for further understanding of EnSC-Exos in the recovery of ovary function.

Background

Premature ovarian failure (POF), which is known as primary ovarian insufficiency (POI) as well, refers to women who are under the age of 40 years old, has amenorrhea and infertility (1). A main cause of POF includes idiopathic factors such as genetics, immunity or iatrogenic (eg: chemotherapy). POF is a devastating diagnosis for reproductive-aged women (2). With the improvement of chemotherapy drugs, the survival rate of cancer patients has been significantly improved, but gonadal damage is still a major complication, and the problem of ovarian damage caused by chemotherapy drugs needs to be resolved urgently (3). Owing to stem cells having self-renewal and regeneration function, they are considered to be effective in treating POF (4). Many studies have demonstrated that stem cells have great potential in

treating infertility caused by female ovarian failure in various animal models and clinical studies (5-7). Human EnSCs, also known as epithelial progenitors and stromal cells, was isolated from endometrial tissues. However, the quality, dosage and delivery route of stem cells must be carefully evaluated (8, 9). Stem cells secrete soluble factors, including extracellular vesicles (EVs), which may influence the microenvironment through paracrine mechanisms (10). Exosomes are nano-scale vesicles that can be used as a medium for cell-to-cell communication (11). In fact, several studies have revealed that exosomes have anti-inflammatory, anti-aging and wound healing effects *in vitro* and *in vivo* models (12). Compared with stem cells, exosomes are more convenient to save and transport. Moreover, they avoid many risks associated with cell transplantation (13). Studies showed that stem cell-derived exosomes can restrain ovarian damage or mitigate fertility decline in mice which was related to age (14). However, the molecular mechanisms, together with the signaling pathways, for improving ovarian function of exosomes needed to be further elucidated.

The Hippo pathway was initially found in the fruit fly drosophila as an intrinsic mechanism that regulates organ size during development and is highly evolutionarily-conserved from drosophila to mammals (15). The Hippo pathway is a growth-supressive kinase cascade that restricts size during development. The core components of the Hippo pathway in mammals consists of a kinase cascade: sterile 20-like kinases (MST1/2), large tumour suppressor kinases (LATS1/2), transcriptional activator Yes-associated protein (YAP) and transcriptional co-activator with PDZ-binding motif (TAZ) (16). MST1/2 can bind to and phosphorylates Sav which is a regulatory, WW-domain containing protein that promotes Lats1/2 phosphorylation, Lats1/2 itself is also a kinase, which phosphorylates and inactivates YAP. The phosphorylated YAP is inactive since it binds to the cytoplasmic scaffold protein 14-3-3, which prevents its nuclear translocation. Otherwise, it enters the nucleus via the nuclear pore, and from there can regulate gene expression (17,18). Recent studies have revealed the Hippo signaling pathway might contribute to development, such as the Hippo signaling is inactivated and YAP and TAZ are activated and free to translocate into the nucleus to regulate target genes involved in cell proliferation, tissue growth, control of organ size and shape or metastasis as mention previously (19). Notably, Hippo pathway is important in folliculogenesis or ovarian function by regulating follicle activation and survival (20). Further investigation revealed that enhanced YAP expression also contributed to massive primordial follicle activation (21). Study shows that disruption of Hippo signaling in the ovary promotes ovarian follicle growth through induction of CCN2 expression (22). At the same time, it has been suggested that disruption of Hippo pathway by BMSCs in ovaries of radiation exposed rats which showed a significant increase in YAP1, TEAD1 genes (23).

Here, we investigated the exogenous EnSC-Exos repressed apoptosis in cisplatin-induced GCs through activating YAP *in vitro* and effectively relieved follicles from atresia in POF mice model through Hippo pathway. Our study indicates the therapeutic potential of EnSC-Exos in chemotherapy-induced POF and the importance of Hippo pathway for POF treatment and thus provides more possible targets for treating POF.

Material And Methods

Isolation of EnSCs

Human endometrial tissues were acquired from the Department of Obstetrics and Gynecology, the First Affiliated Hospital of Xi'an Jiaotong University (Xi'an, Shaanxi, China). The studies involving human participants were reviewed and approved by Ethical Committee of The First Affiliated Hospital of Xi'an Jiantong University. The participants provided their written informed consent to participate in this study. Human endometrial stem cells (EnSCs) were cultured and identified as our previous study described (24). The tissue is placed in glassware under aseptic conditions and cut into $1mm^3$ with ophthalmic scissors and then digested by collagenase type I for 1 hours in a 37℃ rotating shaker. The digestion was terminated using Dulbecco's Modified Eagle Medium/Nutrient Mixture F12 (DMEM/F12, HyClone, USA) complete media and filtered with 200 mesh screen, 400 mesh screen. Finally, the cell-debrispellet was obtained by centrifugation at 800g for 5 minutes. The representative images in this part were captured using a microscope (Olympus Corporation, Tokyo, Japan).

Cell culture

KGN cells were obtained from Wuhan Procell (Procell Life Science&Technology Co., Wuhan, China). The KGN and EnSCs cell lines were cultivated in DMEM/F12 supplemented with 10% fetal bovine serum (FBS, SiJiqing, China). Cells were cultured in 5% CO_2 humidified incubator at 37℃. Human EnSCs were maintained for 3-5 passages in culture, in order to ensure the EnSC-exosomes was fit for experiments.

Exosomes isolation, characterization and labeling

Exosomes were acquired from human EnSCs supernatants by differential centrifugation. In the first place, the medium was thrown away when EnSCs reached 80% confluency. Second, the cells were cultured in DMEM/F12 with 10% exosome-depleted FBS (VivaCell, Cat. no.: C3801-0050, VivaCell Biosciences, Shanghai, China) for another 48 h. The supernatants were gathered and then sequential centrifugation through 300 g for 20 min, 2000 g for 20 min and 10,000 g for 40 min at 4°C in order to filter cells and debris. Then, the supernatants were ultracentrifuged using 120,000 g for 90 min to discard cell supernatant and precipitate was washed using sterile PBS using 120,000 g for 90 min to discard PBS wash solution (Beckman OptimaTM L-80 XP, Beckman Coulter, USA). Finally, the precipitate was suspended in pre-cooled PBS to filtrate through 0.22 μm filters (Millipore, Billerica, MA, United States) (25). The exosome concentrations were determined with a BCA protein assay kit (Proandy, cat. no.:10136-1, Proandy Biotechnology, Shaanxi, China).

To verify the successful isolation of exosomes, Western Blotting (WB) was performed to detect the exosome marker proteins, such as anti-HSP70 (dilution 1:500, cat. no.: sc-32239), anti-Alix (dilution 1:500, cat. no.: sc-53540) and anti-CD81 (dilution 1:500, cat. no.: sc-166029) from Santa Cruz (Santa Cruz Biotechnology, United States); anti-CD9 (D8O1A) (dilution 1:1000, cat. no.: #13174) and β-actin (8H10D10) (dilution 1:5000, cat. no.: #3700) antibodies from Cell Signaling Technologies (Beverly, MA).

Transmission electron microscopy (TEM, hitachi H-7650, Japan) was performed to examine the existence of human EnSC-Exos. Exosomes were dropped onto a carbon-coated copper grid and stained with 2% uranyl acetate for 1 min.

The human EnSCs-Exos were labeled with PKH26 (Sigma-Aldrich, St. Louis, MO, USA) according to the manufacturer's instructions. In short, EnSC-Exos were incubated with equal PKH26 (4 μM) for 4 min at room temperature and treated with equal exosome-depleted FBS to neutralize redundant dye. Finally, the PKH26 labeled exosomes were obtained after centrifuged at 120,000 g for 90 min at 4°C to remove contaminating dye.

Induction of GC apoptosis *in vitro* and coculture of GCs and EnSC-Exos

Cisplatin (Sigma-Aldrich, St. Louis, MO) was used to make the cisplatin-induced the granulosa cell injury model as previous (26). In order to clarify the effect of exosomes to repair granulosa cells (GCs) from cisplatin injury, 1×10^5 GCs were seeded into the of six-well plates and incubate for 24 h. Then the cisplatin (10 μM) was added to the GCs culture medium to induce apoptosis. After exposure to cisplatin for 24 h (10 μM), the GCs were cocultured with human EnSC-exosomes (200 μg/mL) or EnSC-exosomes (200 μg/mL) pretreated with Verteporfin (27) (VP, 1 μM, MedChemExpress, China, catalog no.: HY-B0146) in the system for another 72 h.

For uptake of labeled exosomes, the cisplatin-induced granulosa cell injury model incubation with 10 μg/mL, 200 μg/mL PKH26-labeled exosomes for 24 h. Cells were washed twice with sterile PBS and then fixed in 4% paraformaldehyde for 10 min. After that, the nucleic was stained with 4', 6-diamidino-2-phenylindole (DAPI, Beyotime, cat. no.: P0131, Beyotime Biotechnology, Shanghai, China) and the cytoskeleton was stained with Actin-Tracker Green-488 (Beyotime, cat. no.: C2201S, Beyotime Biotechnology, Shanghai, China) according to the manufacturer's instructions. The uptake of PKH26-labeled exosomes by cisplatin-damaged GCs was observed by the fluorescence microscope (Nikon Ti-S, Nikon Corporation, Japan) and confocal laser scanning microscope (Leica TCS SP5 II, Leica Biosystems, Germany).

Immunofluorescence

Plant the cells on the slides and provide them with different treatments. Cells were washed twice with sterile PBS, and fixed with 4% paraformaldehyde for 15 min. Then, cells were washed in sterile PBS for three times and then 0.5% Triton X-100 (Beyotime, cat. no.: P0096, Beyotime Biotechnology, Shanghai, China) for 30 min. After that they were blocked with 5% BSA for 1 h. Next, they were incubated with primary antibodies (anti-YAP, dilution 1:100, cat. no.: 13584-1-AP, Proteintech, USA), secondary antibodies (Invitrogen) and DAPI (Beyotime, cat. no.: P0131, Beyotime Biotechnology, Shanghai, China). Using a fluorescence microscope (Nikon Ti-S, Nikon Corporation, Japan), images were captured.

Western blot analysis and antibodies

Total protein of different groups was gathered using RIPA/PMSF/PI (100:1:2) lysis buffer according to the manufacturer's instructions and the protein concentration in different groups was calculated using the BCA protein assay kit (Proandy Biotechnology, Shaanxi, China). Total protein was separated by 10% Gels, under 60 V electrophoresis for 40 min, followed by 100 V electrophoresis for 60 min. Then, total protein of different groups after electrophoresis were transferred into a 0.22 μm NC membrane (PALL, Germany) using 320 mA for 100 min. After blocking with 5% non-fat milk in Tris-Buffered Saline and Tween (TBST) for 120 min at room temperature shaker (50 rpm). The membranes were incubated with primary antibody overnight at 4℃ refrigerator. The membrane was then washed with TBST 3 times for 8 min next day, afterwards, the membranes were incubated with secondary antibodies (HRP-labeled, dilution 1:3,000, cat. no.: ZB-2301, ZSGB-BIO, China) for 1.5 h. The membrane was washed 3 times for 10 min with TBST to detect using chemiluminescence detection reagent and Chemiluminescent Imager (Tanon-5200, Shanghai, China). All protein expression levels were normalized to the level of the internal standard control Glyceraldehyde-3-phosphate dehydrogenase (GAPDH, dilution 1:5,000, cat. no.: AP0063, Bioworld Technology, USA). The following antibodies were used for Western blot: anti-Bcl-2 (dilution 1:1,500, cat. no.: 12789-1-AP), anti-Bax (dilution 1:1,500, cat. no.: 50599-2-Ig), anti-MST1 (dilution 1:1,000, cat. no.: 22245-1-AP), anti-LATS1 (dilution 1:1,500, cat. no.: 17049-1-AP) from Proteintech Group (Proteintech, USA); anti-Phospho-MST1 (Thr183)/MST2 (Thr180) (E7U1D) (dilution 1:1,000, cat. no.: #49332) antibody and anti-YAP (D8H1X) (dilution 1:1,000, cat. no.: #14074), anti-Phospho-YAP (Ser127) (D9W2I) (dilution 1:1,000, cat. no.: #13008), anti-Phospho-LATS1 (Ser909) (dilution 1:1,000, cat. no.: #9157), anti-CD9 (D8O1A) (dilution 1:1000, cat. no.: #13174) and β-actin (8H10D10) (dilution 1:5000, cat. no.: #3700) antibodies from Cell Signaling Technologies (Beverly, MA); anti-PCNA (dilution 1:500, cat. no.: sc-56), anti-Caspase-3 (dilution 1:500, cat. no.: sc-7272), anti-HSP70 (dilution 1:500, cat. no.: sc-32239), anti-Alix (dilution 1:500, cat. no.: sc-53540) and anti-CD81 (dilution 1:500, cat. no.: sc-166029) from Santa Cruz (Santa Cruz Biotechnology, United States).

RNA extraction and quantitative real-time PCR (qRT-PCR)

Total RNA of cells was collected using Trizol reagent (Invitrogen, USA) and standardized total RNA (1.8 < A260/A280 < 2.2) was used in experiments. Total RNA (1 μg) was converted into cDNA using the PrimeScript™ RT reagent Kit with gDNA Eraser (Takara, Japan). After that, cDNA was subjected to PCR amplification using TB Green® Premix Ex Taq™ II (Takara) in Bio-Rad CFX (Bio-Rad, United States). The following thermocycling conditions were used for qRT-PCR: 95℃ for 1 min, 39 cycles with 95℃ for 20 sec, 60℃ for 20 sec, 72℃ for 30 sec. GAPDH was used as an internal control. The expressions of genes were quantified using the $2^{-\Delta\Delta Cq}$ method. The primer sequences were as following:

ANKRD1-F: 5'-GCCAAAGACAGAGAAGGAGATAC-3';

ANKRD1-R: 5'-GAGATCCGCGCCATACATAAT-3';

CYR61-F: 5'-CACACCAAGGGGCTGGAATG-3';

CYR61-R: 5'-CCCGTTTTGGTAGATTCTGG-3';

CTGF-F: 5’-GGAAATGCTGCGAGGAGTGG-3’;

CTGF-R: 5’-GAACAGGCGCTCCACTCTGTG-3’;

GAPDH-F: 5'-GTGAAGGTCGGAGTCAACGG-3’;

GAPDH-R: 5'-GAGGTCAATGAAGGGGTCATTG-3’.

Flow cytometry assay

According to the manufacturer’s protocol, cisplatin-induced GCs apoptosis model and EnSC-Exos repair of the cisplatin-induced GCs injury model were determined by flow cytometry using the Annexin V-FITC Apoptosis Detection Kit (BD Biosciences, CA, USA). Briefly, cells were washed with cold PBS twice, then cells stained with Annexin V-FITC (5 μL) and propidium iodide (5 μL) for 15 min at room temperature in darkness. The stained cells were analyzed using flow cytometry (FC 500, MCL, CA) in 1 h.

5-ethynyl-2'-deoxyuridine (EdU) labelling staining

To assess appropriate concentration for EnSC-Exos contribute to cisplatin-damaged GCs repair and the proliferation rate of the cisplatin-induced granulosa cell injury model in different groups, BeyoClick^{TM} 5-ethynyl-2-deoxyuridine (EdU)-594 kit (Beyotime, cat. no.: C0078S, Beyotime Biotechnology, Shanghai, China) was used according to the manufacturer’s instructions. In brief, KGN cells (1×10^4) were cultured in a 96-well plate for 24 h, the cisplatin was added to the GCs culture medium at 10 μM for 24 h to induce apoptosis (the cisplatin-induced granulosa cell injury model), then 100, 200, 400 μg/mL EnSC-Exos were suspended in cisplatin-damaged GCs for 72 h to detect the appropriate concentration for EnSC-exos contribute to cisplatin-damaged GCs repair. To detect the effect of Hippo pathway inhibitor on KGN proliferation in different groups, the GCs were cocultured with EnSC-exosomes (200 μg/mL) or EnSC-exosomes (200 μg/mL) pretreated with Verteporfin (1 μM) in the system for 72 h.

For EdU labelling assay, cells were incubated with EdU (1:1000, 10 μmol/L) for 2 h. Then, KGN cells were fixed with 4% formaldehyde for 15 minutes. Next, permeabilized the cells in 0.5% Triton X-100 (100 μL) for 15 minutes and added the BeyoClick^{TM} Labeled-Azide reaction cocktail (100 μL) for 30 minutes under light-shading conditions at room temperature. Finally, cells were counterstained with Hoechst 33342 (nuclear staining) for 30 minutes at room temperature. After 3 times washes with PBS, the images were acquired using luorescence microscope (Nikon Ti-S, Nikon Corporation, Japan). The proliferation rate of cells was assessed with the proportion of EdU-positive nucleus (red) to blue fluorescent nucleus.

Experimental animals, POF model establishment

To establish the POF model in mice, a total of 40 C57BL/6 female mice aged 6–8 weeks were purchased from Beijing Vital River Laboratory Animal Technology Co., Ltd. The animal study was reviewed and approved by Ethical Committee and the Institutional Animal Care and Use Committee of Xi’an Jiaotong University. The mice were bred in a free condition in a comfortable temperature.

To establish the POF model, mice were injected with cisplatin (2 mg/kg) intraperitoneally for 10 consecutive days (5). To demonstrat the therapeutic effect of EnSC-Exos on POF ovarian function through Hippo pathway, the mice were randomly divided into 4 groups: (1) Control group (n = 10); (2) Cisplatin group (n = 10): cisplatin (2 mg/kg) intraperitoneal injection daily for 10 days; (3) Exosome group (n = 10): cisplatin (2 mg/kg) intraperitoneal injection daily for 10 days, exosome (350 μg/mouse) tail vein injection every other day from 11^{th} day for 6 times; (4) Verteporfin group (n = 10): cisplatin (2 mg/kg) intraperitoneal injection daily for 10 days, Verteporfin (75 mg/kg) intraperitoneal injection every other day from 11^{th} day for 6 times and exosome (350 μg/mouse) tail vein injection every other day from 11^{th} day for 6 times at the same time. The animals were euthanized by cervical dislocation after 22 days of treatment to collect serum and ovaries. We have recorded the body weight of each mouse every day (Figure 5A).

Enzyme Linked Immunosorbent Assay (ELISA)

After 22 days of treatment in different groups, blood collected from mice eyeball was transferred to sterile tube for centrifugation at 4500 r/min for 15 minutes at 4℃ (eppendorf, Germany) to obtain mice serum. Then, anti-Mullerian hormone (AMH), estradiol (E_2) and follicle stimulating hormone (FSH) levels were detected using mice ELISA kit (Meimian Biotechnology, Jiangsu, China) according to the kit instructions.

Hematoxylin-eosin (HE) staining

First, mice ovarian tissues were fixed in 4% paraformaldehyde for 24 h, embedded in paraffin and cut into a 4 μm serial sections. Then, mice ovarian tissue sections were incubated in xylene, dehydration in alcohol gradient of 100%-70% and rehydrated. Finally, mice ovarian tissue sections were stained with hematoxylin and eosin (HE) after deparaffinization.

Immunohistochemistry (IHC)

First, mice ovarian tissues of different groups were fixed in 4% formaldehyde, paraffin-embedded and cut into a 4 μm serial sections. Then, serial sections were deparaffinized with xylenes, rehydrated and retrieved the antigen in sodium citrate solution (pH 6.0) for 20 minutes. After that the slides of the endogenous peroxidase were quenched using 3% hydrogen peroxide and blocked with 1% BSA to block the nonspecific binding for 30 minutes. Then mice ovary tissue sections were incubated with primary antibody anti-YAP (dilution 1:200, cat. no.: 13584-1-AP, Proteintech, USA) overnight at 4℃ refrigerator. The slides were washed using PBS for 5 times and incubate with Secondary antibody (HRP-conjugated, 1:1000, Santa, Cruze) for 1 h. Finally, the DAB substrate kit (Beyotime, Shanghai, China) was applied to detect peroxidase reactivity. DAB peroxidase substrate was prepared in 2 mL ddH_2O in a clean bottle. Then, drop the DAB substrate on top of the slides and observe the brown staining using a microscope. Immerse the slides in tap water to stop the reaction and rinse under cold tap water for 5 min.

Statistical analysis

The statistical analyses were conducted through GraphPad Prism and SPSS. The cell experiments in this article were carried out in triplicate. All results are shown as the mean ± SD. Student's t-test and one-way ANOVA were applied to compare the two experimental groups and multiple groups, respectively. Significance is indicated as following: $P < 0.05$; $^{**}P < 0.01$.

Results

Cultivation and characterization of EnSC-Exos

Human EnSCs passaged 3 to 5 times had a uniform morphologica appearance as fibroblast-like long spindles in an ordered arrangement (Figure 1A). The human EnSCs possessing a multilineage differentiation capability and flow cytometry was used to identify the expression of surface markers as mention previously (28). EnSC-Exos were isolated by differential ultracentrifugation. The average production of exosomes was approximately 10 μg/μL according to protein content. Characteristics of EnSC-Exos were analyzed by electron microscopy, which revealed vesicular structures-circular and double membrane wrapped in shape. At the same time, electron microscopy analysis showed that the size was range 30-150 nm (Figure 1B). Western blot revealed the presence of exosome surface markers including Alix, HSP70, CD81 and CD9 (Figure 1C). This infers that human EnSC-Exos were successfully isolated.

Cisplatin-damaged GCs induce the apoptosis *in vitro* through activating the Hippo signaling pathway

Cisplatin is one of the most potential and widely used drugs for the treatment of various solid cancers such as ovarian, cervical cancer and several others (29). In order to be closer to the actual situation, we chose cisplatin to induce apoptosis of granulosa cells to establish the cisplatin-induced granulosa cell injury model *in vitro* for subsequent experiments. Using 0, 5, 10 or 20 μM of cisplatin concentration induced granulosa cells apoptosis for 24 h was determined by flow cytometry. The apoptotic GCs were counted in each group after staining with Annexin V-FITC and propidium iodide. Figure 2A showed the apoptosis rate of cisplatin-damaged GCs was increased in a dose dependent manner in the concentration range of 0-20 μM. Western blot showed cisplatin efficiently stimulated cell apoptosis in a dose dependent manner and the level of apoptosis protein Bax, Caspase-3 was remarkably up-regulated whereas the expression of anti-apoptosis protein Bcl-2 was distinctly down-regulated in cisplatin-damaged GCs, which leaded to the higher ratio of Bax/Bcl-2 (Figure 2B). These results suggest 10 μM was selected as the optimal concentration for subsequent experiments as mention previously (26).

The MST and LATS are core kinase cascades while YAP and TAZ are downstream effector of the Hippo pathway in mammalian. The core kinase MST phosphorylates, activates LATS and activated LATS phosphorylates YAP at the site of S127, giving a location for 14-3-3 proteins, sequestering YAP in the cytoplasm when the Hippo signaling is activated (30). In the nucleus, YAP/TAZ interacts with TEA DNA-binding protein transcription factors to form the YAP/TAZ-TEAD complex. It mediates factors such as connective tissue growth factor (CTGF), cysteine-rich angiogenic inducer 61 (CYR61), Ankyrin repeat domain 1 (ANKRD1) to stimulate cell survival, proliferation and growth (31). On the contrary,

unphosphorylated YAP translocates acts as a transcriptional coactivator into the nucleus, where it inducing the expression of genes that promote cell proliferation and inhibit apoptosis.

For the purpose of determining whether the expression level of the Hippo pathway core effectors was associated with the cisplatin-induced granulosa cell injury model, we measured the protein expression levels of phospho-MST1 (p-MST1), p-LATS1 (the active form), p-YAP (the inactive form), MST, LATS1 and YAP (the active form) by WB as well as the expression levels of YAP by immunofluorescence, while the YAP target genes were measured using qRT-PCR. We found that treatment of GCs with cisplatin *in vitro* reduced the protein expression levels of LATS1, YAP, and MST and increased the expression levels of p-LATS1, p-YAP, and p-MST1 in a time-dependent manner (Figure 2C). We found that the total RNA levels of the YAP target genes ANKRD1, CTGF and CYR61 were also decreased after cisplatin treatment through qRT-PCR experiments (Figure 2D).

Furthermore, immunofluorescence staining revealed that expression of YAP had a lower level of cytoplasm expression and nucleus accumulation in the cisplatin-damaged GCs, compared to the control group. In addition, the expression level of YAP is decreased as the concentration of cisplatin increases and there is almost no expression of YAP in the cytoplasm and nucleus of 20 μM cisplatin-damaged GCs (Figure 2E). Therefore, these results suggest that cisplatin damage GCs and suppress proliferation of GCs by activating the expression of Hippo/YAP signaling core effectors.

Uptake of EnSC-Exos by cisplatin-damaged GCs *in vitro*

The appropriate concentration for EnSC-exos contribute to the cisplatin-induced granulosa cell injury model (the cisplatin was added to the GCs culture medium at 10 μM for 24 h to induce apoptosis) repair was determined by EdU assay. The results showed that the proliferation rate of cisplatin-damaged GCs treated with 200 or 400 μg/mL EnSC-Exos for 72 h was significantly higher when compared to the 100 μg/mL EnSC-Exos. Thereby, 72 h of incubation with 200 μg/mL EnSC-Exos significantly promoted the proliferation of cisplatin-damaged GCs and were used for subsequent experiments (Figure 3A).

Exosomes are known to be taken up by other cells by endocytosis, triggering cellular responses (32). EnSC-Exos were labeled with PKH26, a fluorescent cell linker compound. To evaluate the internalization of EnSC-Exos, cisplatin-damaged GCs *in vitro* were incubated with 200 μg/mL and 10 μg/mL PKH26 labeled EnSC-Exos for 24 h, which can be observed strong red fluorescence under the fluorescence microscope in the cytoplasm of cells (Figure 3B). Furthermore, when the exosomes concentration was 10 μg/mL, the uptake could be seen by immunofluorescence microscopy in the cisplatin-induced granulosa cell injury model. While under the concentration of 200 μg/mL, EnSC-Exo increased the uptake of fluorescence intensity in cisplatin-damaged GCs. Confocal laser scanning microscope showed clearly that 10 μg/mL PKH26 labeled human EnSC-Exos were located inside the cytoplasmic compartment of cisplatin-damaged GCs (Figure 3 C).

In addition, the red fluorescence decreases after the addition of Hippo pathway inhibitor Verteporfin at 1 μM (Figure 3 B). Verteporfin (VP) is a suppressor of YAP, used as a photosensitizer for photodynamic

therapy in patients with age-related macular degeneration (33). These results suggested that EnSC-Exos could be taken in by cisplatin-damaged GCs and the endocytosis of exosomes was reduced after inhibiting the Hippo signaling pathway *in vitro*.

EnSC-Exos attenuated the apoptosis on cisplatin-damaged GCs by suppressing Hippo pathway *in vitro*

The biological function of EnSC-Exos contributed to cisplatin-damaged GCs was analysed using flow cytometry analysis, western blot and EdU labelling assay. In our research, the apoptosis rates of positive control (Cisplatin group) were significantly higher than negative control (Control group). The apoptosis rate of cisplatin-damaged GCs cocultured with EnSC-Exos (200 μg/mL) for 72 h was decreased, there was significant difference among Cisplatin group and Exosome group, contemporary (Figure 4A). Western blot showed that EnSC-Exos could inhibit the expression of apoptosis protein Bax and promote the expression of proliferation protein PCNA in cisplatin-damaged GCs, the anti-apoptotic effect of EnSC-Exos is reduced after adding Hippo pathway inhibitors -Verteporfin (Figure 4B). Afterwards, proliferation of EnSC-Exos induced cisplatin-damaged GCs was evaluated by EdU labelling assay. The result showed that EnSC-Exos (200 μg/mL) enhanced cell proliferation of the cisplatin-induced granulosa cell injury model. As expected, EnSC-Exos induced growth of cisplatin-damaged GCs was significantly inhibited by the addition of Hippo pathway inhibitor Verteporfin at 1 μM (Figure 4C). All results indicate that human EnSc-Exos could promote the repair of the cisplatin-induced granulosa cell injury model which was associated with Hippo pathway.

Next, the mechanism underneath of Hippo pathway in the therapeutic effects of EnSC-Exos on cisplatin-damaged GCs was detected using western blot analysis, qRT-PCR and immunofluorescence staining. KGN cell lines were maintained in cisplatin (10 μM) for 24 h to establish cisplatin-induced granulosa cell injury model. Then cisplatin-damaged GCs treated with PBS (Cisplatin group), EnSC-Exos (200 μg/mL) (Exosome group) or EnSC-Exos (200 μg/mL) with Verteporfin (1 μM) (Exosome + Verteporfin group) for another 72 h. Western blot indicated that cisplatin could induce YAP phosphorylation, while EnSC-Exos up-regulated the protein expression level of YAP and then decreased phosphorylation of YAP. What is more interesting, cells were treated with Verteporfin and EnSC-Exos for 72 h, the expression of proteins in the Hippo pathway, such as total YAP, p-YAP, LATS1, p-LATS1 and MST1 were inhibited. The results indicate that EnSc-Exos may inhibit cisplatin-damaged GCs apoptosis via the Hippo pathway (Figure 4D). Using qRT-PCR, we found that the total RNA levels of the YAP target genes ANKRD1 and CTGF were increased after EnSc-Exos treatment, while decreased in Exosome and Verteporfin group (Figure 4E).

As shown in Figure 4F, cisplatin could induce YAP phosphorylation and cytoplasmic localization, which was, as expected, decrease nuclear localization, confirming the Hippo pathway was involved in the apoptotic effect of cisplatin-induced granulosa cells. In contrast, EnSC-Exos caused YAP translocated into nucleus. On the other hand, the inhibitor of Hippo pathway (Verteporfin) significantly suppressed exosomes-induced YAP nuclear localization. Taken together, our observations support a physiological role of EnSC-Exos on cisplatin-damaged GCs in Hippo pathway regulation, which means EnSC-Exos could inhibit cell apoptosis in cisplatin-damaged GCs via suppresses the Hippo pathway.

Therapeutic effects of Human EnSC-Exos on premature ovarian failure mice

Mice were injected intraperitoneally with 2 mg/kg cisplatin daily for 10 days to establish the POF model (5). Control group was intraperitoneally injected with saline. On the eleventh day of cisplatin administration, mice were randomly divided into three groups: (1) received PBS (POF group). (2) hEnSC-Exos (passage 3~5, 350 μg/mouse) every other day from the 11^{th} day by tail vein injection (Exosome group). (3) Verteporfin (75 mg/kg) intraperitoneal injection for 6 times as well as human EnSC-Exos tail vein injection every other day from the 11^{th} day at the same time (Verteporfin group). After 12 days, mice were weighed and sacrificed (Figure 5A). As shown in Figure 5B, six days after injection, Exosome group showed significantly increased body weight compared to POF and Verteporfin groups. Body weight from verteporfin-treated mice and POF group were significantly lighten than those from exosome-treated on 12 days after therapeutic. Furthermore, following human EnSC-Exos injection, the serum levels of anti-Mullerian hormone (AMH), estradiol (E_2) were increased but follicle stimulating hormone (FSH) levels were decreased in Exosomes group compared with POF group, while when incorporation of verteporfin during EnSC-Exos repairing in POF model can reduce E_2 and AMH levels and increase FSH levels in the serum (Figure 5C).

To further examine the effects of human EnSC-Exos transplantation on mice ovarian function, mice ovary tissues were analyzed by histologically. The mice ovaries contained numerous healthy follicles at different stages in Control group, while ovaries composed of interstitial cells in a fibrous matrix in the cisplatin-treated chemotherapy group. POF group demonstrated that a significant reduction in the number of primordial, primary, secondary, and mature follicles in mice ovary tissues. Interestingly, human EnSC-Exos injection into the mice of POF group significantly inhibited granulosa cell apoptosis, protected the ovarian vasculature from damage and increased in total number of healthy follicles and decrease of atresia follicles. What's more, abnormal structural, interstitial hyperplasia, severe fibrosis and less number of functional follicles were observed in in veterporfin-treated mice compared with the Exosome group in morphology of mice ovary sections (Figure 5D). Due to the activation of follicles depends on the Hippo pathway, we detected the expression of YAP in the different treatment groups using IHC. Immunohistochemical analysis showed that chemotherapy significantly decreased YAP protein expression in ovaries. However, human EnSC-Exos slightly enhanced YAP expression in injured ovaries, while verteporfin decreased the expression of YAP (Figure 5E). These results indicate that EnSC-Exos have the potential to repair ovarian function in POF mice model through Hippo pathway.

Discussion

Approximately 10% of cancers are present in women under 45 years of age (34). Treatments for cancer of the female reproductive system, such as cisplatin-based chemotherapy, induces ovarian damage, including GCs apoptosis, ovarian vascular damage, resulting in POF, which is also known as ovarian function insufficient (POI) (35). However, though known to cause intermediate gonadal toxicity, it is currently no curative therapy available to reverse the damage to ovarian structure and function caused by chemotherapy in women of reproductive age (36). Oocytes are stored as primordial follicles surrounded

by somatic granulosa cells in the normal ovary. What's more importantly, granulosa cells play a serious role in follicular activation as well as follicular function. Excessive apoptosis of granulosa cells is a key mechanism for follicular atresia (37). It demonstrated that promoting proliferation of GCs can save cisplatin-damaged ovarian structures and functions. Various approaches were used to preserve fertility in women with cancer, such as embryo cryopreservation, mature-oocyte cryopreservation after ovarian stimulation or ovarian tissue, transplantation, and ovarian protection with GnRH-a (34). Up to date, more studies are essential to assess feasibility, safety and efficacy of these fertility-preserving ways and evaluate advanced therapeutic strategies to deliver the effect of ovarian in chemotherapy.

With the progess of regenerative medicine, human stem cell traetment brings new future for POF. Since stem cells have strong self-renewal and regeneration potential, they can be used in treatment of ovarian failure. Because of stem cells have strong self-renewal and regeneration capacity, they are able to be used in therapy of POF. To date, many studies point to the effect of stem cells in ovarian failure animal model treatment, such as mesenchymal stem cells (MSCs), adult stem cells, embryonic stem cells and ovarian stem cells.(38). Although numerous experimental studies have been carried out, the clinical applications of stem cells have many limitations, including lacking cell sources, immunogenicity and moral problems (39). It is urgent to identify the effective components of stem cells in the therapy of POF to avoid potential side effects. Hence, the cell-free therapy, which was used stem cells as a source of therapeutic molecules, could be developed to treat POF disease models. Exosomes secreted by stem cells, which function as messengers between cells, have been studied on the biological effects because they are smaller and easier to produce and have no risk of tumor formation (40). Recently, many studies have reported that exosomes play an significant role in stem cell-mediated repair of tissue function. For instance, human amniotic epithelial cell-derived exosomes (hAEC-exosomes) increased numbers and improved ovarian function in POF mice. In the early stage of transplantation, hAEC-exosomes significantly decreased GCs apoptosis, protected ovarian blood vessels from damage and participated in maintaining the number of primordial follicles in damaged ovaries *in vivo* (41). In the current study, we characterized exosomes secreted by human EnSC *in vitro* (Figure 1). The uptake of EnSC-Exos by cisplatin-damaged GCs was observed by immunofluorescence staining and laser scanning confocal microscope, confirming direct interaction between exosomes and damaged cells (Figure 3). We also provide new evidence that the expression of PCNA was significantly up-regulated by treating the cisplatin-damaged GCs with EnSC-Exos which means exosomes treatment brings about sustained changes in the proliferation and anti-apoptosis of cisplatin-damged cells (Figure 4).

Several studies have shown that granulosa cell apoptosis is a pathogenic factor that accelerates follicular exhaustion and atresia, depending on the Hippo pathway, which is also negatively regulated by follicle development. Studies have shown that chemotherapy leads to abnormal Hippo signaling pathway in the ovary, which is related to the loss of primordial follicles and apoptosis of granulosa cells. Study demonstrated expression of Hippo signaling pathway genes and shows that ovarian fragmentation increases actin polymerization, leads to YAP nuclear translocation and promotes follicular growth in mammalian ovaries (22). Further studies have shown that enhanced YAP expression and increased pro-inflammatory responses also contribute to the activation of massive primordial follicles (42). Previous

studies showed that Hippo signaling pathway was mainly involved in the regulation of ovarian fragmentation which means that ovarian development is closely related to the Hippo pathway (43). Consistent with this, Hippo is down-regulated in many ovarian damaged cells, we propose that EnSC-exosomes treatment attenuates ovarian damage and restores ovarian function in POF which was related to Hippo pathway. To our knowledge, this is the first study to investigate the interaction between human EnSC-Exos which are related to Hippo pathway in POF model (Figure 6). In order to dicover the beneficial effects of EnSC-Exos in restoring ovarian function in POF and the potential mechanisms. We observe the conditions of cisplatin-damaged CGs treated with exosomes or Hippo pathway inhibitor (Verteporfin). The results showed that cell apoptosis decreased under EnSC-Exos and this effect was reversed by Verteporfin. Subsequently, the cytoplasmic and nuclear fractions were isolated to evaluate the translocation of YAP in cisplatin-treated CGs. After exosomes treatment, the translocation from cytoplasmic to nuclear of YAP protein was increased while Hippo pathway inhibitor were decreased.

In addition, we established a POF mice model to further verify the experimental results. We selected 75 mg/kg Verteporfin to establish the POF mice model. In order to observe whether exosomes play a role in ovarian repair after blocking the Hippo pathway, exosomes were injected as usual in order to observe whether verteporfin could block the Hippo pathway as well as exosomes had the ability to repair ovarian function (Figure 5). The abnormal structure, severe fibrosis was observed in the ovary tissues of Verteporfin group and POF group. In contrast, the morphology and structure of the ovary tissues showed recovery with the evidence of decreased fibrosis and increased number of functional follicles at all developmental stages after EnSC-Exos injection (Figure 5D). Immunohistochemistry showed that the expression of YAP increased in the Control and Exosomes groups while decreased in Cisplatin and Verteporfin groups. Based on these results, we demonstrated that exosomes to suppress the Hippo pathway and increases YAP activation to result in anti-apoptosis of cisplatin-damaged CGs and POF model. In our research, all these data provide a potential therapeutic approach to treatment with ovarian injury. However, our study still has some limitations. First, it is needed to verify in a large number of animal experiments whether the dose and time of verteporfin used in cisplatin-induced POF mice model affect the blocking effect of Hippo pathway. Second, regardless of the fact that we observed exosomes could be used in cisplatin-damaged CGs, the molecular mechanism underlying the upstream or the downstream signaling molecule such as RNA, protein and growth factors we did not further investigate. In addition, the therapeutic effect of EnSC-Exos remains to be validated in a clinical trial such as POF patients. All these limitations should be discussed in the future study.

Taken together, human EnSC-Exos were successfully isolated, identified and labeling. Furthermore, we found the Hippo signaling pathway was responsible for the apoptosis of cisplatin-damaged CGs. *In vitro*, co-cultured with EnSC-Exos significantly improved the proliferation levels of cisplatin-damaged GCs. Human EnSC-Exos injection can promote ovarian cells proliferation and restore ovarian function in POF mice model. Furthermore, we found that the therapeutic effect of EnSC-Exos on cisplatin-damaged GCs was inhibited by the Hippo pathway inhibitor-verteporfin in vitro and POF mice model.

Conclusion

Our research shows that human EnSC-Exos can repair ovarian injury, stimulate regeneration and recovery of ovarian function via activating YAP and inhibiting the Hippo signaling pathway. Our findings suggest that EnSC-exosomes could act as an additional mechanism contributing to follicles and improved ovarian function microenvironment which is related to Hippo pathway. Thus, human EnSC-Exos injection may provide an effective and novel method for treating chemotherapy-induced POF.

Abbreviations

AMH: anti-Mullerian hormone; ANKRD1: Ankyrin repeat domain 1; CTGF: connective tissue growth factor; CYR61: cysteine-rich angiogenic inducer 61; EVs: extracellular vesicles; E_2: Estradiol; EdU: 5-ethynyl-2'-deoxyuridine; ELISA: Enzyme-linked immunosorbent assay; EnSCs: Endometrial stem cell; Exos: exosomes; EnSC-Exos: Endometrial stem cell-derived exosomes; FSH: follicle stimulating hormone; HE: Hematoxylin-eosin; IHC: Immunohistochemical; GCs: granulosa cells; GAPDH: glyceraldehyde-3-phosphate dehydrogenase; LATS1: large tumor suppressor 1; MSCs: Mesenchymal stem cells; MSC-exosomes: mesenchymal stem cell-derived exosomes; MST1: mammalian Ste20-like protein kinases 1; POF: Premature ovarian failure; POI: primary ovarian insufficiency; PBS: phosphate-buffered saline; qRT-PCR: quantitative real-time PCR; TAZ: transcriptional coactivator with a PDZ-binding domain; VP: Verteporfin; WB: Western blot; YAP: Yes-associated protein; p-YAP: phospho-YAP;

Declarations

Ethics approval and consent to participate

The collection of the samples used for research purposes in this study was approved by the Ethical Committee of The First Affiliated Hospital of Xi'an Jiantong University and written informed consent was obtained from each donor.

The experimental protocol about animals was approved by the Ethical Committee and the Institutional Animal Care and Use Committee of Xi'an Jiaotong University.

Consent for publication

Not applicable.

Availability of data and materials

All data generated or analysed during this study are included in this published article.

Competing interests

The authors declare that they have no competing interests.

Funding

This study was supported by " the National Natural Science Foundation of China (No. 81571393)", "Shaanxi Provincial Natural Science Foundation (No. 2019 KW-065)" and "Project A of the First Afliated Hospital of Xi'an Jiaotong University (XJTU-2021-02)".

Authors' contributions

YXY, WW and WLJ were in charge of the conception, study design, and literature research. WLJ, YXY, WRL, and WLH were in charge of the experimental studies. WJY, CFY and CZW were in charge of the experimental studies and data analysis/interpretation. WW, WLJ and WJY were in charge of manuscript preparation and editing and revision and final version approval of the manuscript. All authors read and approved the ending version of the final manuscript.

Acknowledgements

We thank the support of Center for Translational Medicine, the First Affiliated Hospital of Xi'an Jiaotong University, China. All authors are acknowledged for their contribution to the study.

References

1. Ghahremani-Nasab M, Ghanbari E, Jahanbani Y, Mehdizadeh A, Yousefi M. Premature ovarian failure and tissue engineering. J Cell Physiol. 2020;235(5):4217–26.
2. Blumenfeld Z. What Is the Best Regimen for Ovarian Stimulation of Poor Responders in ART/IVF? Front Endocrinol (Lausanne). 2020;11:192.
3. Cho HW, Lee S, Min KJ, Hong JH, Song JY, Lee JK, et al. Advances in the Treatment and Prevention of Chemotherapy-Induced Ovarian Toxicity. Int J Mol Sci. 2020;21(20).
4. Zhang C. The Roles of Different Stem Cells in Premature Ovarian Failure. Curr Stem Cell Res Ther. 2020;15(6):473–81.
5. Yoon SY, Yoon JA, Park M, Shin EY, Jung S, Lee JE, et al. Recovery of ovarian function by human embryonic stem cell-derived mesenchymal stem cells in cisplatin-induced premature ovarian failure in mice. Stem Cell Res Ther. 2020;11(1):255.
6. Bahrehbar K, Rezazadeh Valojerdi M, Esfandiari F, Fathi R, Hassani SN, Baharvand H. Human embryonic stem cell-derived mesenchymal stem cells improved premature ovarian failure. World J Stem Cells. 2020;12(8):857–78.
7. Ding L, Yan G, Wang B, Xu L, Gu Y, Ru T, et al. Transplantation of UC-MSCs on collagen scaffold activates follicles in dormant ovaries of POF patients with long history of infertility. Sci China Life Sci. 2018;61(12):1554–65.
8. Esfandyari S, Chugh RM, Park HS, Hobeika E, Ulin M, Al-Hendy A. Mesenchymal Stem Cells as a Bio Organ for Treatment of Female Infertility. Cells. 2020;9(10).

9. Shareghi-Oskoue O, Aghebati-Maleki L, Yousefi M. Transplantation of human umbilical cord mesenchymal stem cells to treat premature ovarian failure. Stem Cell Res Ther. 2021;12(1):454.
10. Batsali AK, Georgopoulou A, Mavroudi I, Matheakakis A, Pontikoglou CG, Papadaki HA. The Role of Bone Marrow Mesenchymal Stem Cell Derived Extracellular Vesicles (MSC-EVs) in Normal and Abnormal Hematopoiesis and Their Therapeutic Potential. J Clin Med. 2020;9(3).
11. Kim YG, Choi J, Kim K. Mesenchymal Stem Cell-Derived Exosomes for Effective Cartilage Tissue Repair and Treatment of Osteoarthritis. Biotechnol J. 2020;15(12):e2000082.
12. Ha DH, Kim HK, Lee J, Kwon HH, Park GH, Yang SH, et al. Mesenchymal Stem/Stromal Cell-Derived Exosomes for Immunomodulatory Therapeutics and Skin Regeneration. Cells. 2020;9(5).
13. Wu P, Zhang B, Shi H, Qian H, Xu W. MSC-exosome: A novel cell-free therapy for cutaneous regeneration. Cytotherapy. 2018;20(3):291–301.
14. Jiao W, Mi X, Qin Y, Zhao S. Stem Cell Transplantation Improves Ovarian Function through Paracrine Mechanisms. Curr Gene Ther. 2020;20(5):347–55.
15. Hong AW, Meng Z, Guan KL. The Hippo pathway in intestinal regeneration and disease. Nat Rev Gastroenterol Hepatol. 2016;13(6):324–37.
16. Ma S, Meng Z, Chen R, Guan KL. The Hippo Pathway: Biology and Pathophysiology. Annu Rev Biochem. 2019;88:577–604.
17. Meng Z, Moroishi T, Guan KL. Mechanisms of Hippo pathway regulation. Genes Dev. 2016;30(1):1–17.
18. Huang J, Wu S, Barrera J, Matthews K, Pan D. The Hippo signaling pathway coordinately regulates cell proliferation and apoptosis by inactivating Yorkie, the Drosophila Homolog of YAP. Cell. 2005;122(3):421–34.
19. Dey A, Varelas X, Guan KL. Targeting the Hippo pathway in cancer, fibrosis, wound healing and regenerative medicine. Nat Rev Drug Discov. 2020;19(7):480–94.
20. Gershon E, Dekel N. Newly Identified Regulators of Ovarian Folliculogenesis and Ovulation. Int J Mol Sci. 2020;21(12).
21. Kawamura K, Cheng Y, Suzuki N, Deguchi M, Sato Y, Takae S, et al. Hippo signaling disruption and Akt stimulation of ovarian follicles for infertility treatment. Proc Natl Acad Sci U S A. 2013;110(43):17474–9.
22. Hsueh AJW, Kawamura K. Hippo signaling disruption and ovarian follicle activation in infertile patients. Fertil Steril. 2020;114(3):458–64.
23. El-Derany MO, Said RS, El-Demerdash E. Bone Marrow-Derived Mesenchymal Stem Cells Reverse Radiotherapy-Induced Premature Ovarian Failure: Emphasis on Signal Integration of TGF-β, Wnt/β-Catenin and Hippo Pathways. Stem Cell Rev Rep. 2021;17(4):1429–45.
24. Wang Z, Wang Y, Yang T, Li J, Yang X. Erratum to: Study of the reparative effects of menstrual-derived stem cells on premature ovarian failure in mice. Stem Cell Res Ther. 2017;8(1):49.

25. Théry C, Amigorena S, Raposo G, Clayton A. Isolation and characterization of exosomes from cell culture supernatants and biological fluids. Curr Protoc Cell Biol. 2006;Chap. 3:Unit 3.22.
26. Wang R, Wang W, Wang L, Yuan L, Cheng F, Guan X, et al. FTO protects human granulosa cells from chemotherapy-induced cytotoxicity. Reprod Biol Endocrinol. 2022;20(1):39.
27. Wang L, Li J, Wang R, Chen H, Wang R, Wang W, et al. NGF Signaling Interacts With the Hippo/YAP Pathway to Regulate Cervical Cancer Progression. Front Oncol. 2021;11:688794.
28. Wang Z, Wang Y, Yang T, Li J, Yang X. Study of the reparative effects of menstrual-derived stem cells on premature ovarian failure in mice. Stem Cell Res Ther. 2017;8(1):11.
29. Ghosh S. Cisplatin: The first metal based anticancer drug. Bioorg Chem. 2019;88:102925.
30. Yuan P, Hu Q, He X, Long Y, Song X, Wu F, et al. Laminar flow inhibits the Hippo/YAP pathway via autophagy and SIRT1-mediated deacetylation against atherosclerosis. Cell Death Dis. 2020;11(2):141.
31. Dimri M, Satyanarayana A. Molecular Signaling Pathways and Therapeutic Targets in Hepatocellular Carcinoma. Cancers (Basel). 2020;12(2).
32. Gruenberg J, Stenmark H. The biogenesis of multivesicular endosomes. Nat Rev Mol Cell Biol. 2004;5(4):317–23.
33. Fusco P, Mattiuzzo E, Frasson C, Viola G, Cimetta E, Esposito MR, et al. Verteporfin induces apoptosis and reduces the stem cell-like properties in Neuroblastoma tumour-initiating cells through inhibition of the YAP/TAZ pathway. Eur J Pharmacol. 2021;893:173829.
34. Dolmans MM, Donnez J. Fertility preservation in women for medical and social reasons: Oocytes vs ovarian tissue. Best Pract Res Clin Obstet Gynaecol. 2021;70:63–80.
35. Meirow D, Nugent D. The effects of radiotherapy and chemotherapy on female reproduction. Hum Reprod Update. 2001;7(6):535–43.
36. Sonigo C, Beau I, Binart N, Grynberg M. The Impact of Chemotherapy on the Ovaries: Molecular Aspects and the Prevention of Ovarian Damage. Int J Mol Sci. 2019;20(21).
37. Quirk SM, Cowan RG, Harman RM, Hu CL, Porter DA. Ovarian follicular growth and atresia: the relationship between cell proliferation and survival. J Anim Sci. 2004;82 E-Suppl:E40-52.
38. Sheikhansari G, Aghebati-Maleki L, Nouri M, Jadidi-Niaragh F, Yousefi M. Current approaches for the treatment of premature ovarian failure with stem cell therapy. Biomed Pharmacother. 2018;102:254–62.
39. Fu YX, Ji J, Shan F, Li J, Hu R. Human mesenchymal stem cell treatment of premature ovarian failure: new challenges and opportunities. Stem Cell Res Ther. 2021;12(1):161.
40. Esfandyari S, Elkafas H, Chugh RM, Park HS, Navarro A, Al-Hendy A. Exosomes as Biomarkers for Female Reproductive Diseases Diagnosis and Therapy. Int J Mol Sci. 2021;22(4).
41. Zhang Q, Sun J, Huang Y, Bu S, Guo Y, Gu T, et al. Human Amniotic Epithelial Cell-Derived Exosomes Restore Ovarian Function by Transferring MicroRNAs against Apoptosis. Mol Ther Nucleic Acids. 2019;16:407–18.

42. Gao J, Song T, Che D, Li C, Jiang J, Pang J, et al. Deficiency of Pdk1 contributes to primordial follicle activation via the upregulation of YAP expression and the pro–inflammatory response. Int J Mol Med. 2020;45(2):647–57.
43. Ai A, Xiong Y, Wu B, Lin J, Huang Y, Cao Y, et al. Induction of miR-15a expression by tripterygium glycosides caused premature ovarian failure by suppressing the Hippo-YAP/TAZ signaling effector Lats1. Gene. 2018;678:155–63.

Figures

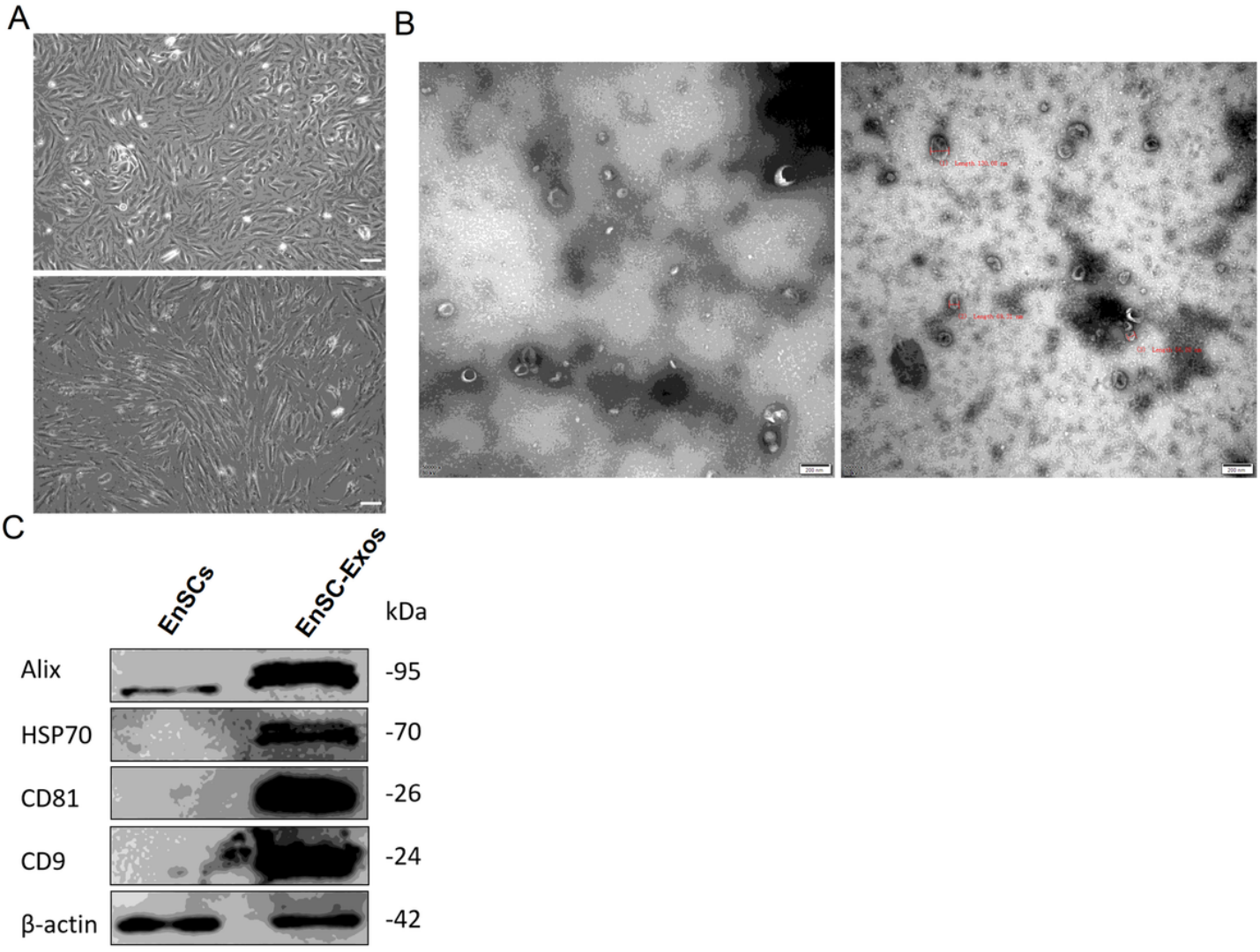

Figure 1

Isolation and identification of EnSC-Exos

(A) First (up panel) and third generation (down panel) EnSCs exhibited a typical fibroblastic morphology. Scale bar: 20 μm. (B) Exosomes isolated from human EnSCs conditioned medium were evidenced by electron microscopy. Scale bar: 200 nm. (C) Western blot analysis of Alix, HSP 70, CD81 and CD9 expression in EnSCs and EnSC-Exos. β-actin was used as a loading control.

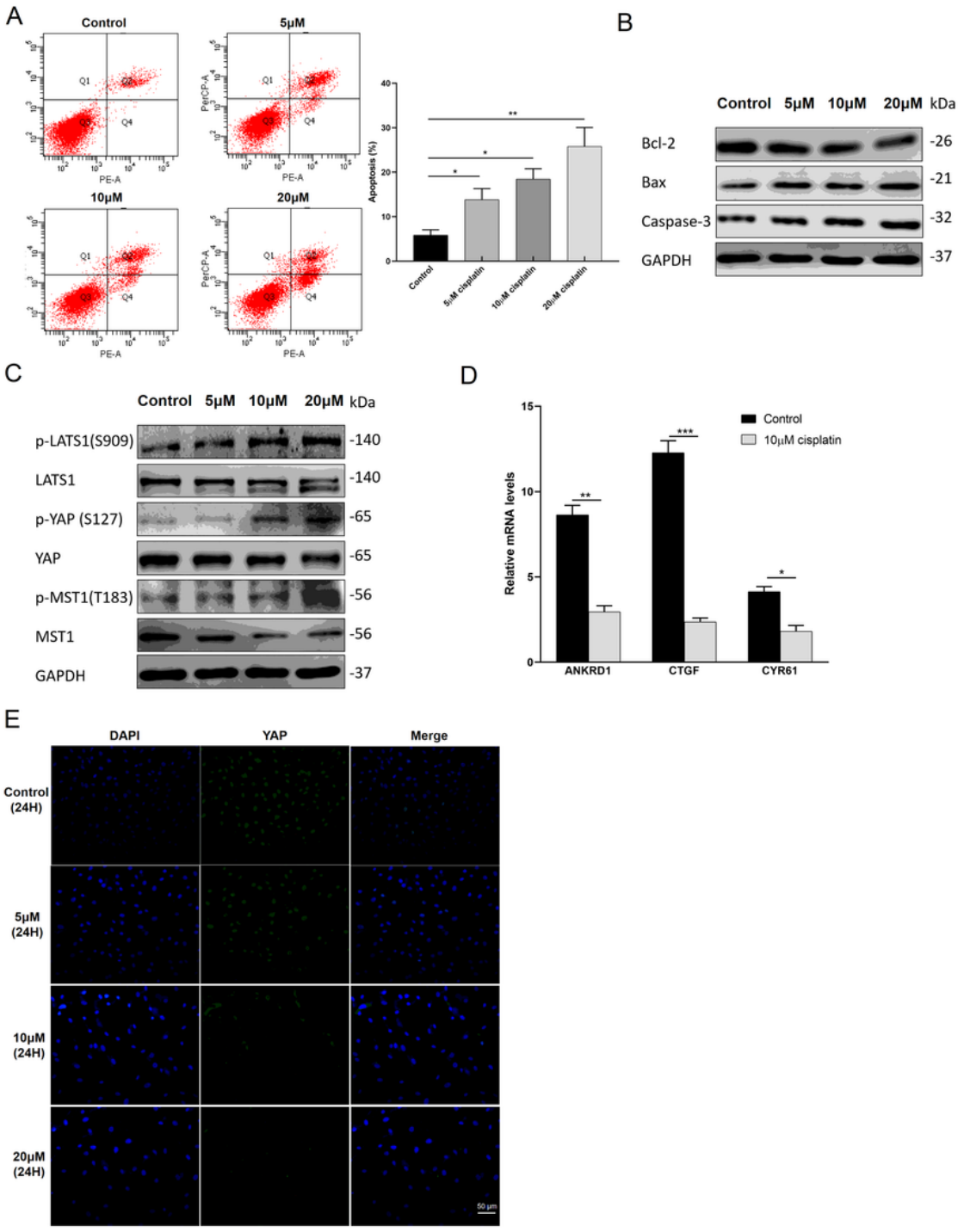

Figure 2

Cisplatin-damaged GCs induce the apoptosis *in vitro* through activating the Hippo signaling pathway

(A) Comparison of apoptotic rates of granulosa cells (GCs) between the groups by flow cytometry (left panel). Comparison of the percentages of apoptotic GCs in each group (right panel). Error bars represent SDs, $^{*}P < 0.05$, $^{**}P < 0.01$. (B) Western blot analysis of lysates with cisplatin-damaged GCs for 0, 5, 10 or 20 μM for 24 h with anti-Bcl-2, anti-Bax and anti-Caspase-3 antibodies. GAPDH was used as a loading control. (C) Cells were cultured in complete medium containing cisplatin (0, 5, 10, 20 μM) for 24 h. Western blot analysis of lysates from different groups with anti-p-LATS1, anti-LATS1, anti-p-YAP, anti-YAP, anti-p-MST anti-MST1 antibodies. GAPDH was used as a loading control. (D) Total RNA expression (qRT-PCR) of YAP target genes between Control group and Cisplatin group (cisplatin-damaged GCs for 10 μM for 24 h). Error bars represent SDs, $^{*}P < 0.05$, $^{**}P < 0.01$, $^{***}P < 0.001$. (E) Immunofluorescence staining indicating that expression of YAP is decreased in cisplatin-damaged GCs, compared to the Control group (YAP was stained with green, Nuclei were stained with blue). Scale bar: 50 μm.

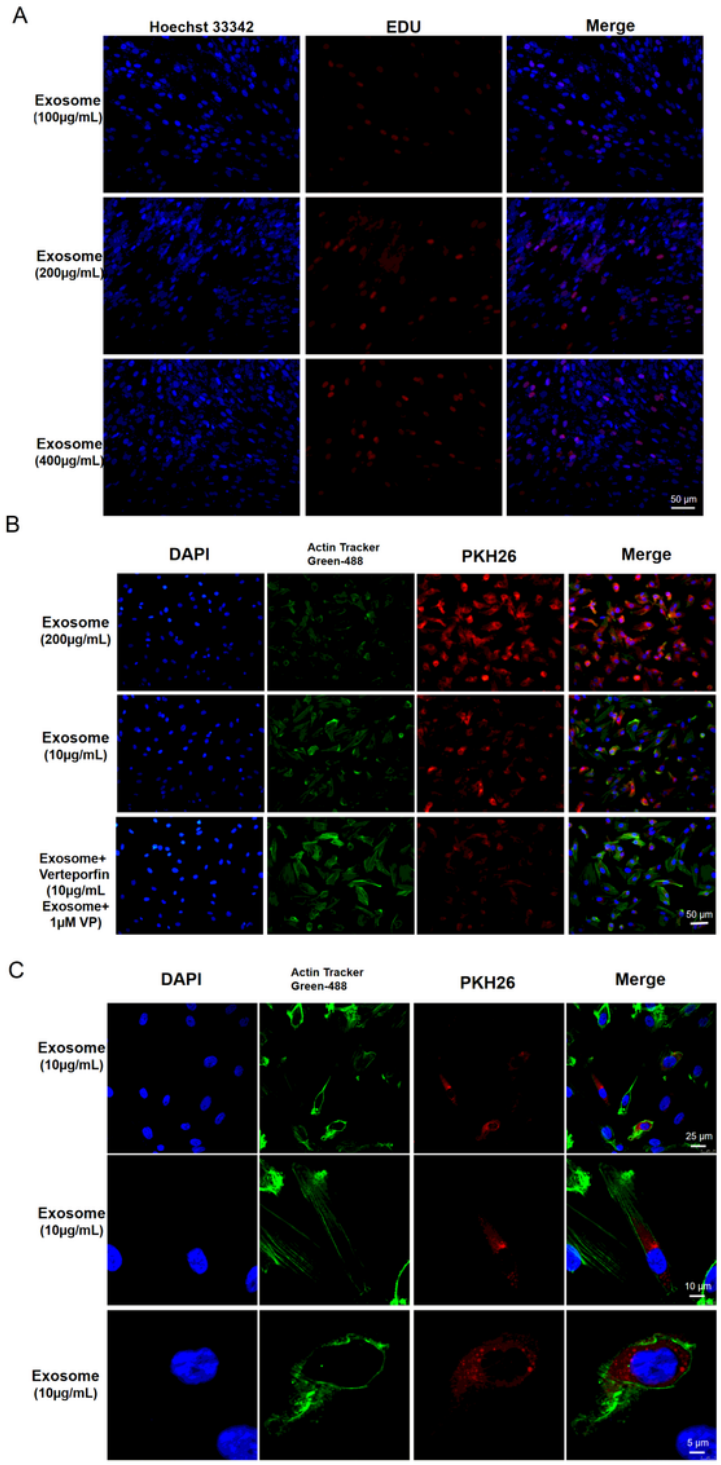

Figure 3

Uptake of EnSC-Exos by cisplatin-damaged GCs

(A) Cell proliferation was determined by EdU labelling. EdU labelling analysis showed the fluorescence images of cisplatin-damaged GCs stimulated with 100, 200, 400 μg/mL EnSC-Exos and detected at 72 h after treatment (EdU, red fluorescent signals; DAPI, blue signals). Scale bar: 50 μm. (B) PKH26 labeled

exosomes were added along with or without Hippo inhibitor-Verteporfin and incubated at 37°C for 24 hours. Uptake of PKH26 labeled EnSC-Exos (red) in cisplatin-damaged GCs was evaluated with fluorescence microscopy. Cytoskeleton was stained with Actin-Tracker Green-488 (green). Nuclei were stained with DAPI (blue). Scale bar: 50 μm. (C) PKH26 labeled exosomes were added and incubated at 37°C for 24 hours. Uptake of 10 μg/mL PKH26-labeled EnSC-Exos (red) in cisplatin-damaged GCs was detected with confocal laser scanning microscope. Cytoskeleton was stained with Actin-Tracker Green-488 (green). Nuclei were stained with DAPI (blue).

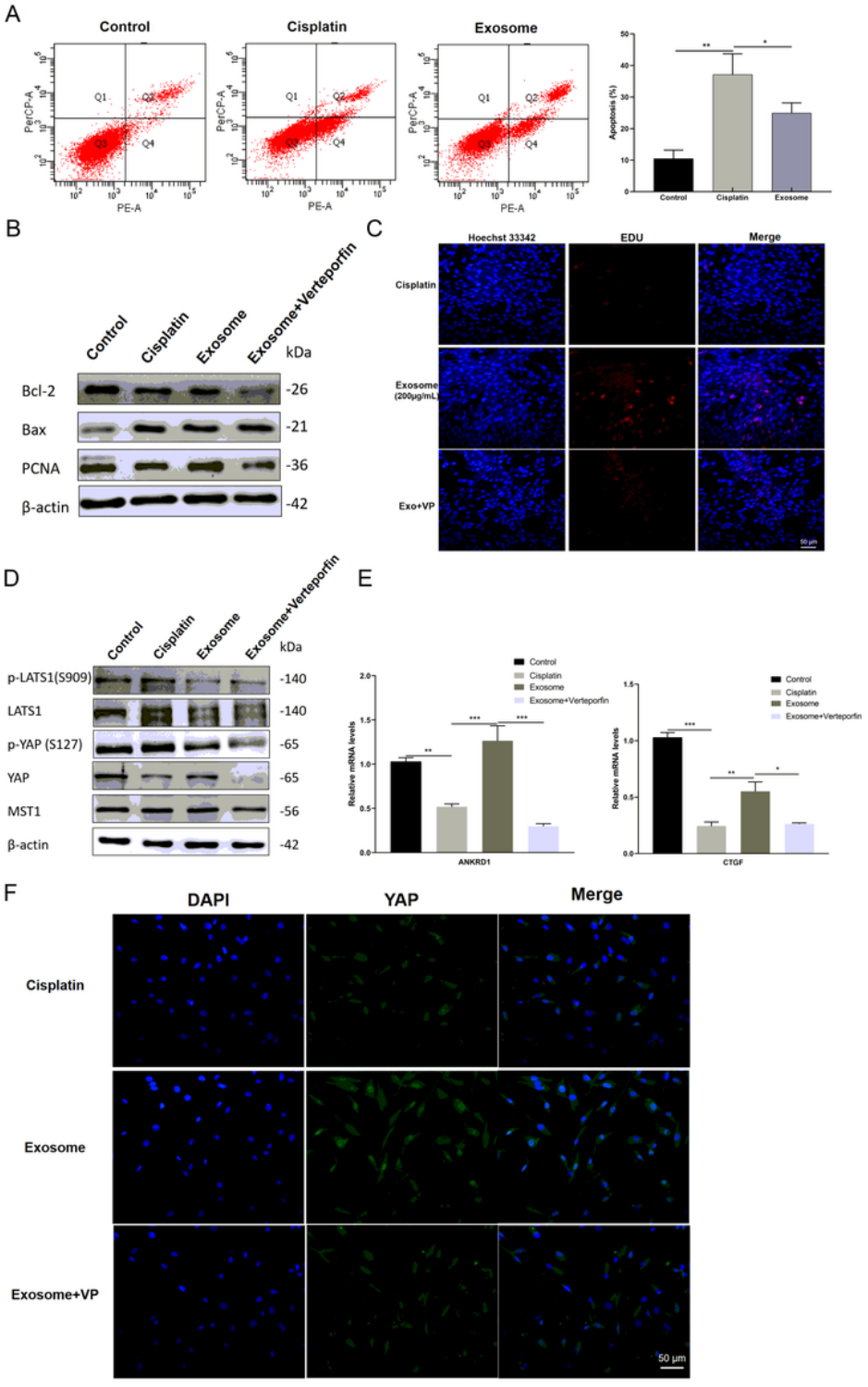

Figure 4

EnSC-Exos attenuated the apoptosis on cisplatin-damaged GCs by suppressing Hippo pathway *in vitro*

(A) The cell apoptosis assay was determined using flow cytometry analysis after the indicated treatment in different groups (left panel). Comparison of the percentages of apoptotic GCs in each group (right panel). Error bars represent SDs, $^{*}P < 0.05$, $^{**}P < 0.01$. (B) Western blot analysis of lysates compared with Control group, Cisplatin group, Exosome group and Exosome + Verteporfin group with anti-Bcl-2, anti-Bax and anti-PCNA antibodies. β-actin was used as a loading control. (C) Cell proliferation was determined by EdU labelling in different groups. EdU labelling analysis showed the fluorescence images of cisplatin-damaged GCs treatment with PBS (Cisplatin group), 200 μg/mL EnSC-Exos (Exosome group) and 200 μg/mL EnSC-Exos with 1 μM Verteporfin (Exosome + Verteporfin group) for 72 h (EdU, red fluorescent signals; DAPI, blue signals). Scale bar: 50 μm. (D) Western blot analysis of lysates from different groups with anti-p-LATS1, anti-LATS1, anti-p-YAP, anti-YAP and anti-MST1 antibodies. β-actin was used as a loading control. Cells were cultured in complete medium containing cisplatin (10 μM) for 24 h before treatment with PBS (Cisplatin group), 200 μg/mL EnSC-Exos (Exosome group) and 200 μg/mL EnSC-Exos with 1 μM Verteporfin (Exosome + Verteporfin group) for another 72 h. (E) Total RNA expression (qRT-PCR) of YAP target genes between different groups. Error bars represent SDs, $^{*}P < 0.05$, $^{**}P < 0.01$, $^{***}P < 0.001$. (F) Immunofluorescence staining indicating that exosomes caused YAP translocated into nucleus while Verteporfin significantly suppressed exosomes-induced YAP nuclear localization (YAP was stained with green, Nuclei were stained with blue). Scale bar: 50 μm.

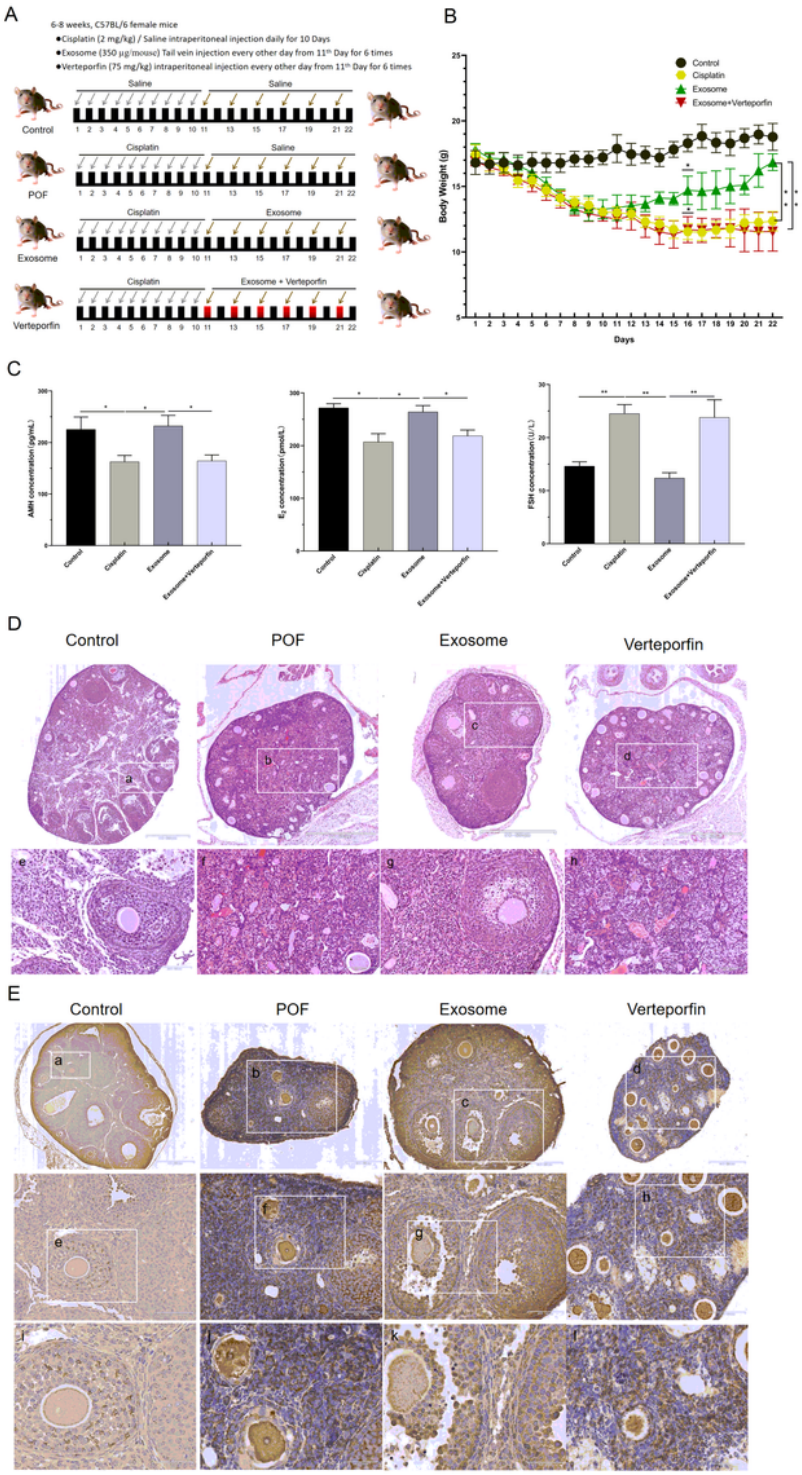

Figure 5

Diagram of the potential mechanisms involved in the effects of EnSC-Exos on cisplatin-induced GCs through Hippo pathway

(A) Schematic description of the experimental design. Cisplatin (2 mg/kg) was administered by intraperitoneal injection for 10 days. On day 11, human EnSC-Exos (350 μg/mouse) were transplanted by

tail vein injection. Verteporfin (75 mg/kg) intraperitoneal injection every other day from 11th Day for 4 times. Experimental analyses were performed after 3 weeks (22^{th}). (B) Body weight were measured each day in different groups. Error bars represent SDs, $^{*}P< 0.05$, $^{**}P< 0.01$. (C) The serum levels of AMH, E_2 and FSH in different groups. Data presented as mean ± SD. $^{*}P< 0.05$, $^{**}P< 0.01$. (D) Representative photomicrographs of H&E-stained ovarian sections in different groups. Scale bar = 4 × 500 μm (Control group) or 5 × 500 μm (POF, Exosome, Verteporfin group). Images e, f, g and h are magnifications of the squares in images a, b, c and d respectively. Scale bar = 20 × 100 μm (Control, POF, Exosome, Verteporfin group). (E) Representative photomicrographs of IHC analysis on YAP in ovarian tissue of mice in different groups. Photomicrographs show hematoxylin and DAB-stained ovaries. Brown in cytoplasm indicates positive expression of the YAP. Blue represents cell nuclear staining. Scale bar = 4 × 500 μm (Control group) or 10 × 200 μm (POF, Exosome, Verteporfin group); Images e, f, g and h are magnifications of the squares in images a, b, c and d respectively. Scale bar = 20 × 100 μm (Control, POF, Exosome, Verteporfin group); Images i, j, k and l are magnifications of the squares in images e, f, g and h respectively. Scale bar = 40 × 50 μm (Control, POF, Exosome, Verteporfin group).

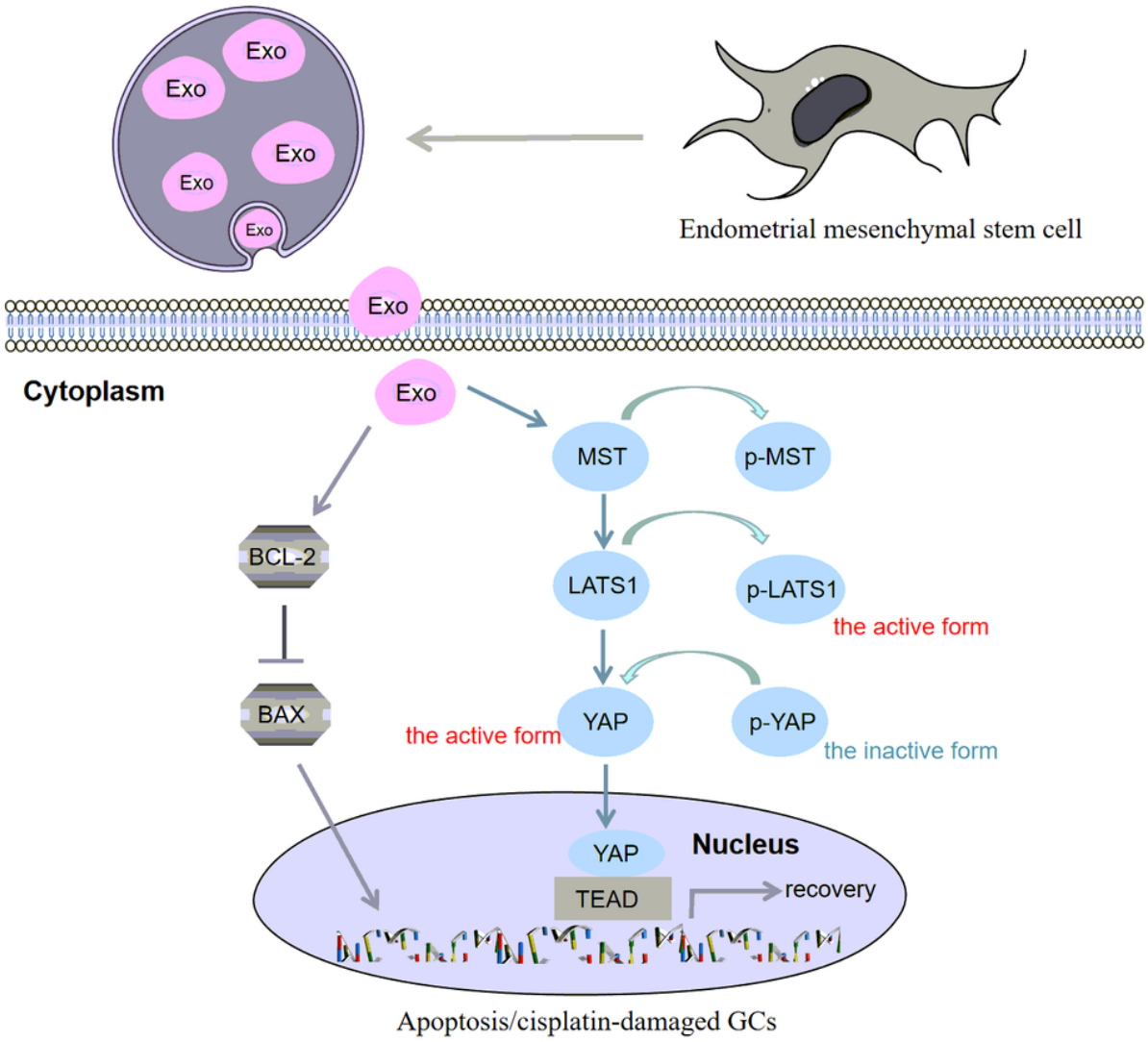

Figure 6

Diagram of the potential mechanisms involved in the effects of EnSC-Exos on cisplatin-induced GCs through Hippo pathway